Journal of Anatomy

J. Anat. (2008) **212**, pp853–862 doi: 10.1111/j.1469-7580.2008.00904.x

Collagenous microstructure of the glenoid labrum and biceps anchor

A. M. Hill,[1] E. J. Hoerning,[1] K. Brook,[1] C. D. Smith,[1] J. Moss,[2] T. Ryder,[2] A. L. Wallace[3,4] and A. M. J. Bull[1]

[1]*Department of Bioengineering, Imperial College London, UK*
[2]*Department of Histopathology, Imperial College London, UK*
[3]*The Shoulder Unit, Hospital of St. John & St. Elizabeth, London, UK*
[4]*Department of Musculoskeletal Surgery, Imperial College London, UK*

Abstract

The glenoid labrum is a significant passive stabilizer of the shoulder joint. However, its microstructural form remains largely unappreciated, particularly in the context of its variety of functions. The focus of labral microscopy has often been histology and, as such, there is very little appreciation of collagen composition and arrangement of the labrum, and hence the micromechanics of the structure. On transmission electron microscopy, significant differences in diameter, area and perimeter were noted in the two gross histological groups of collagen fibril visualized; this suggests a heterogeneous collagenous composition with potentially distinct mechanical function. Scanning electron microscopy demonstrated three distinct zones of interest: a superficial mesh, a dense circumferential braided core potentially able to accommodate hoop stresses, and a loosely packed peri-core zone. Confocal microscopy revealed an articular surface fine fibrillar mesh potentially able to reduce surface friction, bundles of circumferential encapsulated fibres in the bulk of the tissue, and bone anchoring fibres at the osseous interface. Varying microstructure throughout the depth of the labrum suggests a role in accommodating different types of loading. An understanding of the labral microstructure can lead to development of hypotheses based upon an appreciation of this component of material property. This may aid an educated approach to surgical timing and repair.

Key words confocal microscopy; glenoid labrum; scanning electron microscopy; transmission electron microscopy.

Introduction

The glenoid labrum supplies nutrition to the glenoid cavity and maintains joint lubrication (Williams et al. 1995). It contributes to the passive stability of the glenohumeral joint through a variety of mechanisms, acting as an attachment site for capsuloligaments, biceps and triceps (Hertz et al. 1986; Levine & Flatlow, 2000) and as a chock-block, preventing the humeral head from slipping (Matsen et al. 1991). It also increases the scapular articular surface area in contact with the humeral head by approximately one third (Hertz et al. 1986; Levine & Flatlow, 2000) and protects the chondral surface from compression and shear damage (Williams et al. 1995; Nishida et al. 1996). Finally, acting as a valve, the labrum seals the joint from atmospheric pressure, thus maintaining negative intra-articular pressure; any labral lesion would break this seal, which could possibly increase joint instability and cartilage strains in the glenohumeral joint (Habermeyer et al. 1992; Ferguson et al. 2001).

Labral lesions are implicated in the pathophysiology of shoulder instability (Tamai et al. 1986; Cooper et al. 1992; Pagnani & Warren, 1994; Bigliani et al. 1995; Pagnani et al. 1995; Levine & Flatow, 2000; Wasserlauf & Matava, 2003) and surgical repair of such labral lesions is imperative to alleviate pain, prevent recurrent instability and thus restore shoulder function (Hertz et al. 1986).

The organization, orientation and type of collagen fibres in the glenoid labrum and its surrounding structures play a significant role in the material properties of the complex. Microscopically, there are differing views on the exact histological composition of the labrum. Some studies describe the labrum as a fibrocartilaginous structure defined as a dense cartilaginous fibrous tissue with chondrocytes (Prodromos et al. 1990; Williams et al. 1995; Nishida et al. 1996), whereas others describe the labrum as a fibrous structure with a small fibrocartilaginous transition zone between the hyaline cartilage and the fibrous

Correspondence
Dr Anthony M.J. Bull, Department of Bioengineering, Imperial College London, Room B436, Level 4, Bessemer Building, South Kensington Campus, London SW7 2AZ, UK. T: +44 20 75945186; F: +44 20 75846897; E: a.bull@imperial.ac.uk

Accepted for publication *2 March 2008*

labral tissue (Moseley & Övergaard, 1962; Cooper et al. 1992; Huber & Putz, 1997). However, it is known that there is a temporal relationship of labral histology with fibrillation of the labral articular surface and the intercellular matrix within the 4th decade of life (Prodromos et al. 1990).

The core structure of the labrum is composed of densely packed collagen fibre bundles that run in a circumferential orientation around the glenoid rim (Hertz et al. 1986; Tamai et al. 1986; Gohlke et al. 1994; Nishida et al. 1996; Huber & Putz, 1997). These circumferential collagen fibres intermingle where the biceps tendon inserts into the superior aspect of the labrum (Hertz et al. 1986; Cooper et al. 1992) with some radially orientated fibres (Nishida et al. 1996), found more precisely as radial superficial fibre bundles in the anterior and upper labral regions (Huber & Putz, 1997). With high resolution microscopy, Nishida et al. (1996) identified an additional superficial layer composed of a thin, wrinkled woven, mesh-like matrix of fine fibril networks and a middle multilayered stratified zone approximately 200 μm thick consisting of different patterns of fibrillar bundles aligned parallel to the glenoid rim, with interconnecting fibrils. Sharpey's fibres were also identified anchoring the labrum to the superficial layer of the bone. An earlier study identified a superficial layer of randomly arranged fibres, a deep layer consisting of compact bundled circumferential fibres, and sparse regions of radially oriented fibre anchors penetrating cartilage and bony glenoid (Tamai et al. 1986). Huber & Putz (1997) identified fibre bundles running obliquely towards the scapula neck with radial bending of bundles before insertion into the subchondral bone at an acute angle. Finally, in contrast to the distinction of labral histological compartments, study with polarized light microscopy has demonstrated that the organization of the collagen fibres is more haphazard in the labrum than in the capsule (Nishida et al. 1996).

The material properties of a structure are a component of its mechanical behaviour and, as such, understanding elements that in concert compose these properties may develop our understanding of how the labrum functions as a stabilizer in the shoulder joint (Hertz et al. 1986). In application, through understanding the mechanical function and collagen orientation of the glenoid labrum, a better appreciation of when and how to repair it in patients suffering from clinical shoulder instability may be gleaned.

The aim of this study was to investigate the orientation and arrangement of the collagen fibres and the type of collagen in the glenoid labrum with the use of scanning electron microscopy (SEM), confocal microscopy and transmission electron microscopy (TEM). From this data, hypotheses will be developed to deepen our understanding of labral functional anatomy, and also guide quantitative computational and numerical modelling of the structure.

Methods

Specimen preparation

Five fresh frozen cadaveric shoulders (56–91 years old, 2♀:3♂) without glenohumeral joint pathology were used. Specimens were harvested with approval from the local Research Ethics Committee and consent from the donors' next of kin. The specimens were stored at –20 °C and thawed at room temperature for 24 h prior to arthroscopy and dissection.

Shoulders were grossly harvested via an extended superficial deltopectoral skin incision. The specimens were divided through the deep deltopectoral interval; the origin of coracobrachialis and short head of biceps were elevated from the tip of the coracoid, and reflected distally. The osteotendinous junction at the humeral head of the subscapularis musculotendinous unit was then divided and reflected off the anterior capsule. The insertional rim of the capsule onto the humerus was incised to disarticulate the glenohumeral joint. The articular surface of the glenoid was osteotomized at 5 mm deep to the glenoid bare-area enabling the labrum to be micro-sectioned *ex situ*, whilst not damaging the capsulolabral insertion about the rim of the glenoid.

The specimens were sectioned under loupes by sharp dissection radially from the centre of the glenoid outwards into 17 distinct segments, so that each specimen included articular cartilage with subjacent bone, labrum and capsule. The specimens were then fixed in 4% paraformaldehyde (PFA). Labral specimens from three shoulders were randomly allocated for electron microscopy analysis and the specimens from the final two specimens were used for confocal microscopy.

Transmission electron microscopy

TEM specimens were fixed with 3% glutaraldehyde at 4 °C and replaced by 0.1 M cacodylate buffer. These were further dissected under a dissecting microscope into longitudinal strips no greater than 1 mm in width, fixed for 4 h in 3% glutaraldehyde at 4 °C, then saturated in 0.1 M cacodylate buffer for 30 min. Osmium tetroxide 1% was added to post-fix the specimens and left for 1 h before washing. Aqueous uranyl acetate 2% was added for 30 min to block stain the specimen, before dehydrating with increasing concentrations of ethanol to absolute. The specimens were infiltrated and embedded in Spurr's epoxy resin in a polythene rubber mould and polymerized at 70 °C overnight. The embedded specimens were mounted on a pedicule under light microscopy to optimize estimates of obliquity, sectioned on an ultra-microtome (Ultra-Cut, Reichert, NY) and stained with toluidene blue. The samples were then laid upon a copper disk grid and stained with aqueous uranyl acetate 1% and Reynolds lead citrate, before visualization under TEM. Electron micrographs of one area within a grid window with transverse collagen fibres were taken. In this way, 15 grid windows were randomized and photographed at a magnification of ×11 000 for image analysis. The negatives were then developed and enlarged by a factor of 9. Ten of these images that were the most suitable for image analysis were selected.

Upon initial inspection of the TEM images, there were two grossly distinct groups of fibril morphologies. This is a similar finding to authors describing the collagenous architecture of scar formation in ligaments (Hill et al. 2006), inherited connective tissue dysplasias (Ghadially, 1997), rheumatoid tissue (Neurath, 1993) and shoulder and elbow capsules from normal subjects (Kaltsas, 1983). Whilst there is a suggestion that these fibrils relate

to collagen type, and different collagen types contribute to the mechanics of the labrum (Tamai et al. 1986), no such correlation has been purposefully drawn here. However, whatever the aetiology of collagen geometry, there is good reason to suggest an increase in diameter of collagen fibrils leads to an increase in the tensile strength of the tissue (Parry & Craig, 1977). For this reason, it was thought appropriate to view these observed groupings as independent for the purpose of comparing histomorphometric parameters in this mechanical context, with the understanding that this might be mis-representing a range of phylogenetically identical fibrils. The photographic images were digitized. Each common fibril was encircled in red, and the uncommon fibrils (stellate and spiral) in blue to compare them in the image analysis program (KS300, Imaging Associates Ltd, UK). The parameters measured were regional data for individual fibrils: minimum diameter, area, perimeter and circular shape factor (relative similarity function between the minor and major axes of a circular cross-section). The two fibril types were compared for each of the above variables using Student's unpaired *t*-test with an alpha value of 0.05 (SPSS 11.5 for Windows, SPSS Inc.).

Scanning electron microscopy

Specimens for SEM were immersed in buffered formalin and stored at 4 °C until required for processing. Orientation of each specimen was maintained throughout the following process.

Each specimen was rapidly cooled in liquid N_2 along with a brass fracture plate and blade for 5 min. A thermoinsulating polystyrene type guillotine was used to aid positioning of the blade more easily over a clamped specimen, and keep the blade cool during the positioning process. Each segment was cryo-cut perpendicular to the articular surface (transverse section) in a radial manner. The mirror image transverse section was refrozen and cryofractured longitudinally through the deep layer of the labrum. To compare two cryofractured edges, the second fracture was propagated longitudinally from the scalpel cut side towards the cryo-cut side (Fig. 1). Once fractured, the specimen was placed in 4% paraformaldehyde to thaw, and stored for 24 h at 4 °C.

The segments were rinsed with 2 M NaOH and then treated in 2 M NaOH for 4 days at room temperature to remove the extracellular matrix and expose the details of the fine collagen fibre networks (Ohtani et al. 1988, 1992). The specimens were rinsed twice and stored in distilled water for 3 days at room temperature. Following this, the specimens were treated in 1% tannic acid solution for $1^1/_2$ h to improve the preservation of surfaces by structural reinforcement of the collagen fibres (Owen et al. 1999), and rinsed twice. The specimens were fixed in 1.0% OsO_{O4} for 1 h, dehydrated using increasing concentrations of ethanol to absolute, and critically point dried in liquid CO_2 (POLARON, Watford, UK). The specimens were mounted on an aluminium stub using silver paint in amyl acetate and air dried. The specimens were coated with gold using a gold target T8847 40 mm × 0.1 mm in an Emscope SM 300 (Emitech Ltd, Ashford, Kent, UK) sputter chamber. Each specimen was then individually examined under the Scanning Electron Microscope (Cambridge S360 SEM) and digitally imaged (Dell Optiplex 100cx personal computer) with a Prysm frame grabber (Synoptics, Cambridge) and AcQuis image processing software (Synoptics, Cambridge). Each labral segment was imaged through a series of increasing magnification in areas of interest identified on primary inspection.

Confocal laser scanning microscopy

Confocal laser scanning microscopy specimens were frozen in Cryo-M-Bed using liquid nitrogen and mounted onto a cryostat chuck. This was achieved by placing the specimen in a plastic mould embedded on the Cryo-M-Bed before floating the mould in liquid N_2 until frozen. After allowing the tissue to equilibrate in the cryostat (Cryotome E, Shandon, UK) for 10 min, circumferential sections of varying thickness were cut (8 μm, 10 μm, 12 μm, 15 μm) between −20 °C and −25 °C. The sections were thaw mounted onto poly-L-lysine-coated microscope slides (BDH laboratory supplies) and stored at −80 °C. Cut specimen slides were selected from the superficial, middle and deep regions of the tissue, thawed, stained with Haematoxylin and Eosin (H&E) for 2 min, dehydrated, and coverslipped with XAM mounting medium (Gurr, BHD Laboratory Supplies, UK).

Radial sections were either prepared and stained using the same method, or wax embedded. Wax embedding required dehydration of the tissue through an ethanol series to absolute, washing twice in Xylene for 5 min, infiltrating in wax at 60 °C before embedding in fresh wax on a mount. Radial sections of varying thickness (5–15 μm) were cut using a Sledge Microtome and disposable blades. These specimens were stained with H&E and either propidium iodide or anti-vimentin antibody stain. Propidium iodide staining was carried out over 30 s following a phosphate-buffered saline (PBS) rinse, and then washed with distilled water. Anti-vimentin labelling required equilibration in PBS for 5 min, followed by treatment with 0.1% trypsin for 30 min and a further PBS rinse. Following this, a block in 1% bovine serum albumin in PBS for 30 min was conducted before primary antibody incubation (anti-vimentin mouse monoclonal antibody, clone Vim

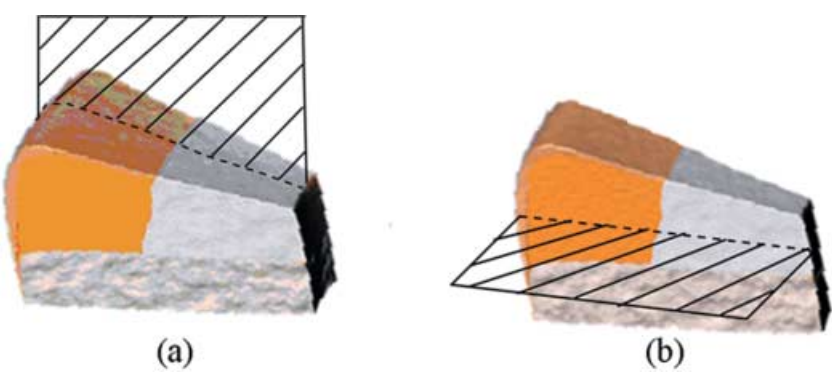

Fig. 1 Labral machining. (a) Radial direction of cryofracture. (b) Mirror image transverse section to (a) refrozen and cryofractured longitudinally through the deep labral core.

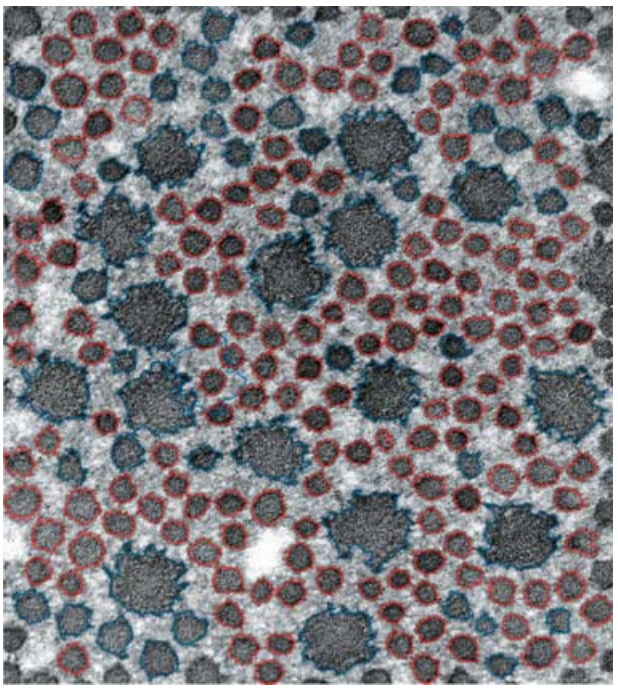

Fig. 2 Transmission electron microphotograph. Two distinct collagen fibre populations are represented; red signifies those that are circular in cross-section, blue are those that consisted of either spiral-shaped fibrils with curved processes, or stellate fibrils with evenly distributed processes.

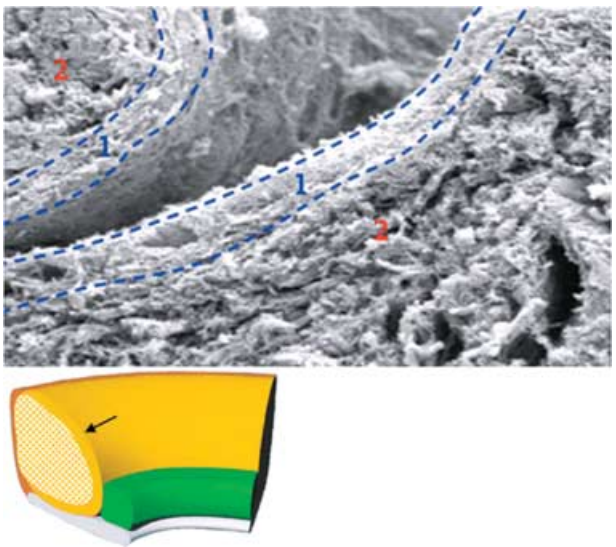

Fig. 3 Superficial scanning electron micrograph. Two apposing superficial fine woven regions (region 1) in a superficial articular surface cleft. Deep to this is the loosely packed, well vascularized region (region 2).

3B4 at a dilution of 1 μg mL^{-1}). Once incubated, the specimen was washed in PBS three times before treatment with the secondary antibody (Dako 1 : 50 anti-mouse conjugated fluorescein isothiocyanate, FITC) and incubated for 1 h at room temperature. Finally, the specimen was washed three times in PBS and then mounted and coverslipped.

Sections were examined using light microscopy and sections chosen for confocal imaging; sections were illuminated at a wavelength of 488 nm (Argon laser) and z series images recorded using the ×10 objective lens and the FITC filter set (BioRad 650 Confocal, BioRad Microscience, UK). With a ×10 objective lens, images were recorded for montage maps from each of the radial and circumferential sections (Leica TCS SP Confocal microscope), and rebuilt *in silico* (Adobe Photoshop Version 6, Adobe System Ltd). Areas of interest were further investigated using ×20 and ×40 objective lenses and z series stacked images recorded.

Results

One specimen had a SLAP II lesion. However, the tissue required for this study was viable in all cases.

Electron microscopy

The circular fibrils with an evenly distributed process had a smaller diameter, area and perimeter than the spiral or stellate fibrils ($P < 0.05$, Fig. 2).

SEM demonstrated three distinct zones: a superficial mesh (Fig. 3), a dense circumferential braided core (Fig. 4), and a loosely packed region surrounding the core (Fig. 5). The superficial surface is a multidirectional fine fibrillar

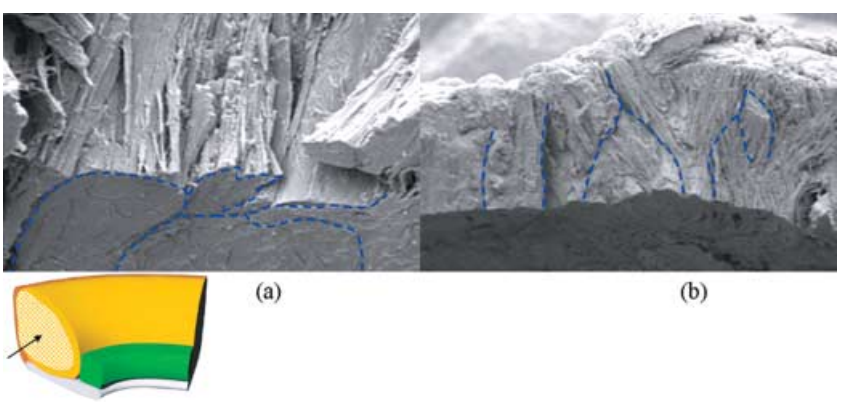

Fig. 4 Scanning electron micrograph of a cryofractured cross-section. (a) Clustered bundles in an oblique view of a cross-section with cryofractured superior surface. (b) Woven arrangement of a similar region viewed on the cryofractured surface.

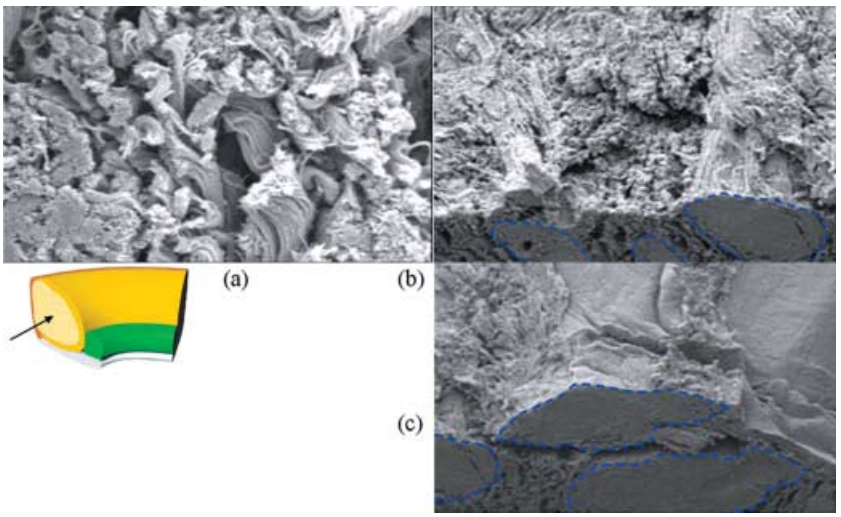

Fig. 5 Scanning electron micrograph at high magnification. (a) High magnification view of the loosely packed collagenous region with a significant amount of crimp. (b,c) Packing arrangement of this region in apposition to the densely packed core region (outlined in blue).

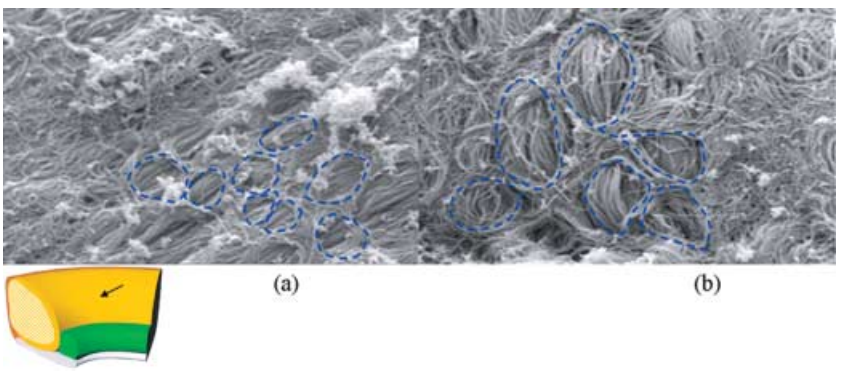

Fig. 6 Scanning electron micrograph of cryofractured surface. (a,b) Fish-net type encapsulation of the core bundles on cryofractured regions

mesh approximately 5–10 μm in depth. Deep to this layer are circumferentially oriented loose fibres with a crimped pattern. This region is often vascularized, most commonly in the superoanterior region of the labrum, but infrequently in the anterior, anteroinferior and posterosuperior regions. The central core is the largest region of the labrum, containing many circumferentially oriented large dense fibre bundles with numerous straight fibrils that run in parallel. This region is relatively avascular. The bundles seemingly were woven or braided around one another, although a similar configuration is not seen within the bundles themselves; the fibres align in parallel within the bundles. These bundles are encapsulated by a fine fishnet-type mesh (Fig. 6).

The labrum attaches to the bone by vertical, oblique and interweaving fibres, in addition to Sharpey's fibres inserting onto the superficial bony surface (Fig. 7). The chondrolabral margin is attached, in addition to Sharpey's fibres, by finger-like processes through foramen in the superficial hyaline cartilage (Fig. 8). The region of apposition between labrum and cartilage is cellular, suggesting a transitional zone between the two materials.

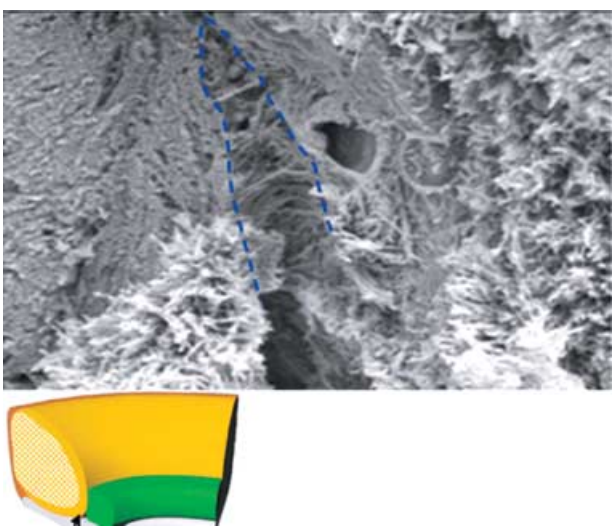

Fig. 7 Scanning electron microphotograph of Sharpey's fibres. A randomly arranged meshwork of Sharpey's fibres exaggerated in a cleft between labrum and boney insertion.

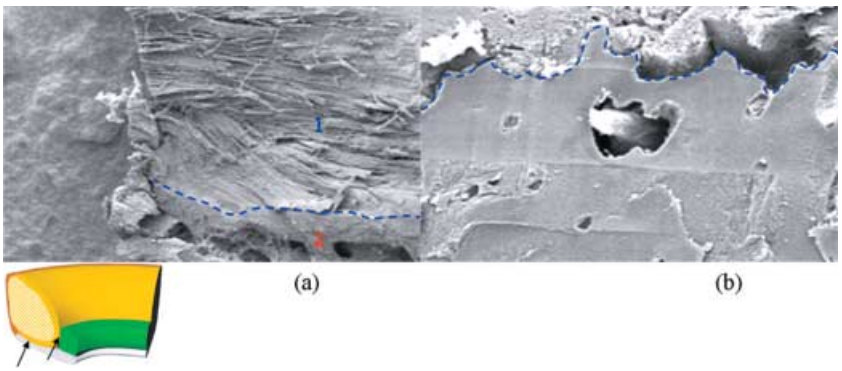

Fig. 8 Scanning electron micrograph of the labral-chondral interface. (a) Cryofractured labral core blending with the bony structure deep to it. (b) Interdigitating finger-like process extruding through a cryofractured chondral surface.

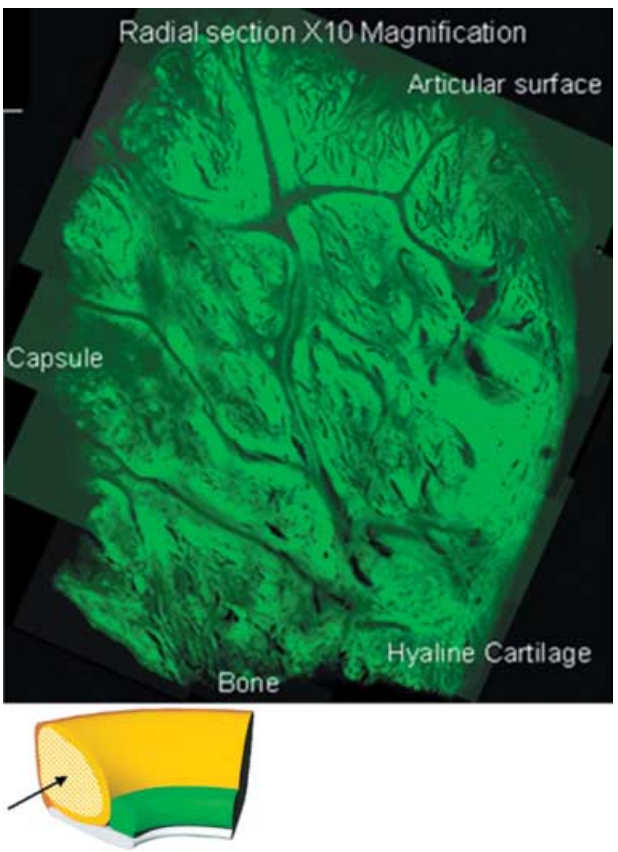

Fig. 9 Confocal microscopic montage of ×10 magnification transverse radial sections taken from a clockwise cross-sectional slide mounted specimen. The entire labral cross-section is represented.

Finally, the biceps tendon inserts into the labrum in a variety of ways on the SEM. However, without exception, the tendon fuses both with the labral structure in a seamless manner, and into its subjacent osseochondral foundation material. Often, the anchor spans a significant portion of labrum.

Confocal microscopy

Of the transverse radial sections, four main zones were identified (Fig. 9). First, on the articular surface, there is a covering of loosely packed fine fibrils with no set orientation (Fig. 10) and a folded region where the capsular tissue inserts, whilst through the middle of the tissue, there are channels of finely packed small fibrils. In the main bulk of the tissue, bundles of densely packed circumferential fibres are encapsulated by loosely packed fibrils (Fig. 10). Near the bone, anchoring fibres are present. However, a number of alternate patterns were seen with the circumferential sectioning (Fig. 11). A fine meshwork of thin fibrils in random orientations, both perpendicular and parallel to the bony surface (Fig. 11), in addition to areas of dividing radial fibres were seen interspersed between sheaths of more densely packed short thicker fibres (Fig. 11) forming a meshwork with fibres in random orientations (Fig. 11), occasionally at 45° to the axis of tissue (Fig. 11), but mainly orientated in densely packed circumferential bundles running along the axis of the tissue.

Propidium iodide staining was used to determine whether there were any cell nuclei present in the tissue, as haematoxylin staining was not successful at demonstrating such structures under light or confocal microscopy. An even distribution of nuclei was seen throughout the radial sections (Fig. 12), although through the centre of the tissue, there seems to be higher densities of cellular material in the loosely packed interdigitating fibrils, often in line with the course of the collagen fibres. This is akin to the vascular distribution seen in the SEM specimens.

Although propidium iodide is able to stain cell nuclei, it is nonspecific for the cell type present. Anti-vimentin antibody (monoclonal antibody to vimentin from mouse-to-mouse hybrid cells-clone Vim 3B4-Boehringer Mannheim) demonstrates the presence of cells of a mesenchymal origin, including endothelial cells, vascular smooth muscle cells, connective tissue cells, all types of blood cells and permanent cell lines, such as fibroblasts. Radial sections stained with anti-vimentin antibody highlighted the cellular structures that had previously been demonstrated by propidium iodide staining. Although the antibody used was not entirely specific, the structure of labelled cells is very suggestive of fibroblasts with finger-like cytoplasmic processes (Fig. 12).

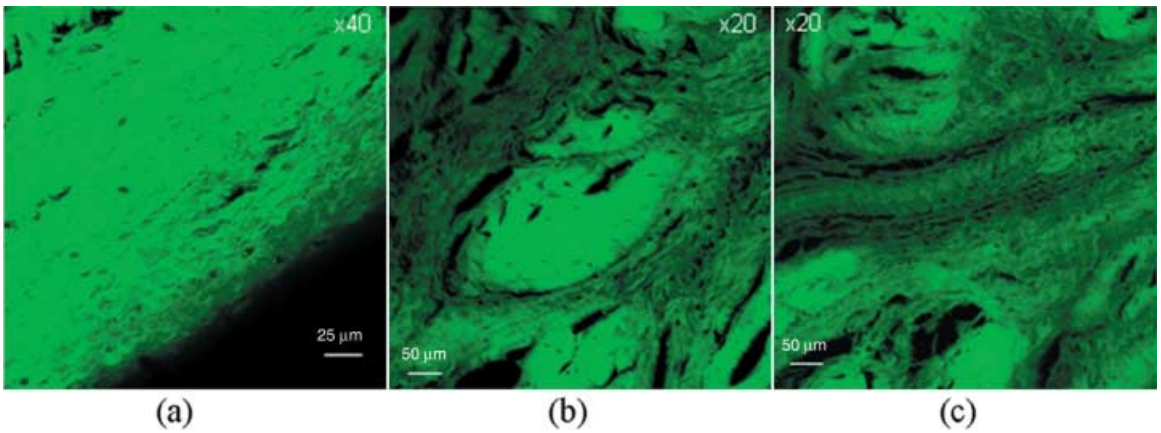

Fig. 10 Confocal microscopic high resolution study. (a) High magnification loosely packed fine fibrils with no set orientation. (b,c) Finely packed small fibrils in apposition to dense fibre bundles.

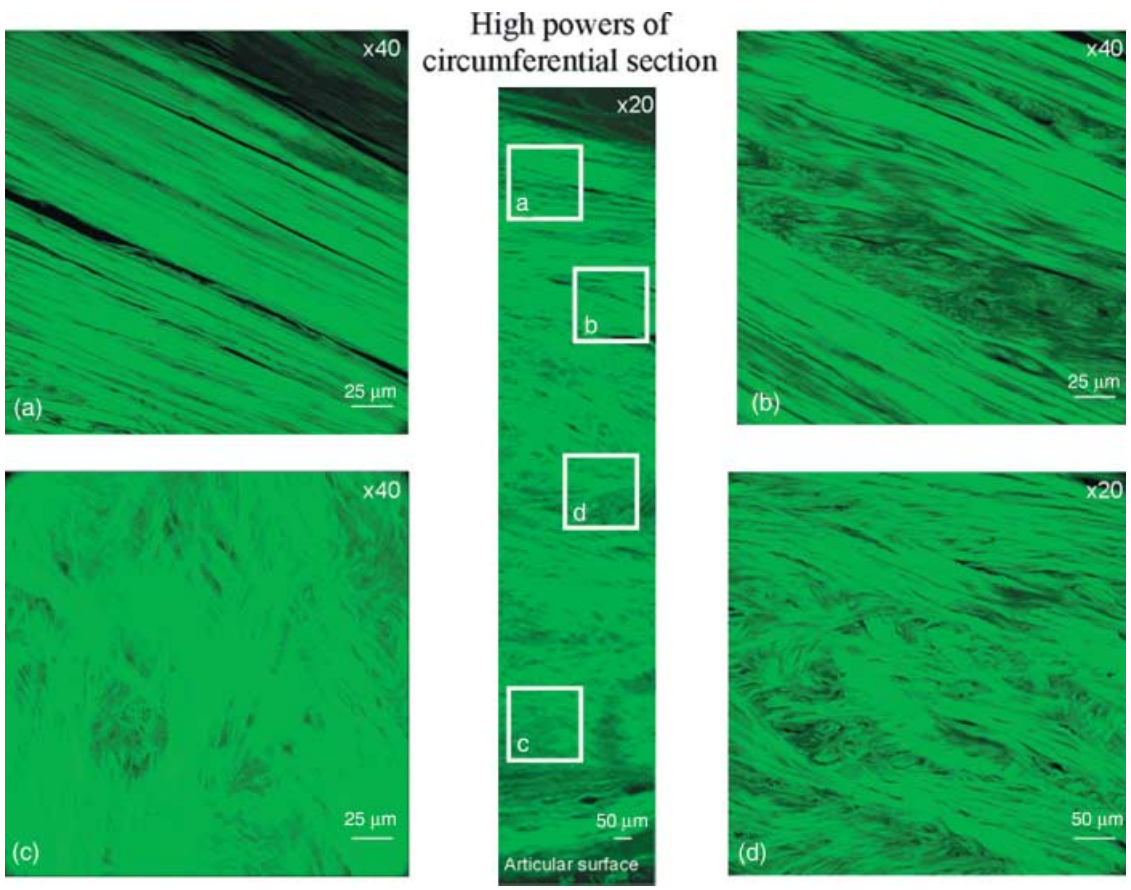

Fig. 11 High resolution confocal study of a circumferential section. These images represent findings from a circumferential section taken at about 2 mm in depth from the superficial labral surface. (a) Densely packed short thicker fibres. (b) Meshwork with fibres. (c) Thin fibrils in random orientations. (d) Fibres oriented occasionally at 45° to the axis of tissue (at a magnification of ×20).

Discussion

The glenohumeral joint is required to achieve a wide range of functions, such as deepening the relatively shallow glenoid cavity, leading to increased resistance to translation of the humeral head by providing a force that centres the humeral head on the glenoid, increasing the surface area of contact for the humeral head, protecting the edges of the bone, assisting in joint lubrication, acting as a suction cup and providing an area of attachment for

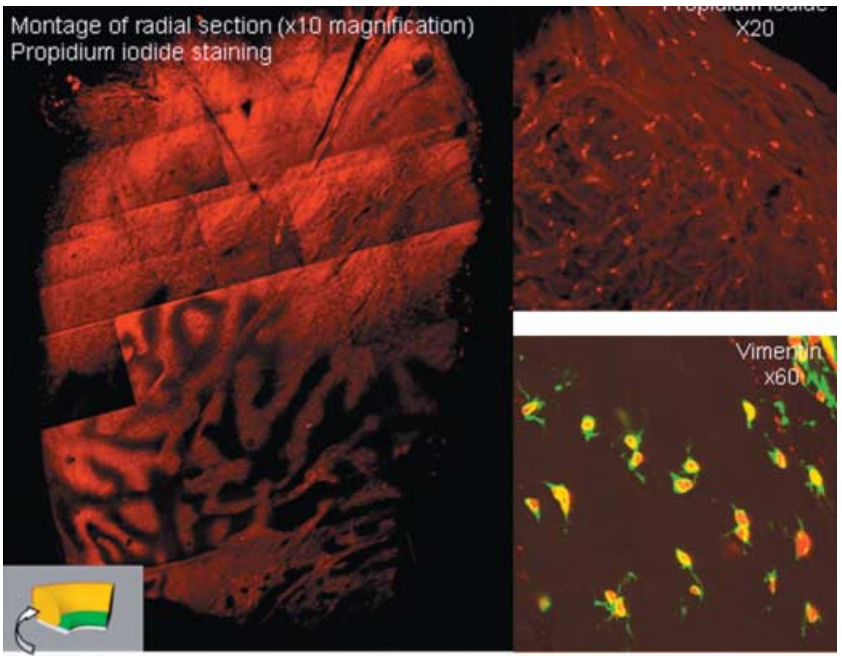

Fig. 12 Confocal microscopy with propidium iodide and anti-vimentin antibody staining. The labral cross-sections demonstrate labelled cells suggestive of fibroblasts with finger-like cytoplasmic processes.

the glenohumeral ligaments and biceps tendon (Pagnani et al. 1995; Fehringer et al. 2003; Rao et al. 2003). The long head of the biceps tendon may act as a tension brace by transmitting force over a wider area by acting as a buttress against humeral head translation (Huber & Putz, 1997), thus reducing contact pressure. As the labrum incorporates the biceps anchor, loads imposed through such a mechanism also require accommodation. The labrum has also been described to vary in its shape according to the different rotational shapes of the humerus (Moseley & Övergaard, 1962). Thus, in deformation, the labrum may have differing functional properties. As such, the structure is subject to a number of different loading conditions, and is thus required to function under a variety of external forces.

The varying microstructure throughout the depth of the labrum also suggests that the labrum plays a role in constraining such a multitude of loading conditions to prevent damage to other structures. Most superficially, the mesh type articular surface of the labrum, whilst subject to a variety of loads, most probably contributes to the reduction in surface friction through lubrication. As the SEM protocol degraded all but the collagen microstructure of the specimen, and the confocal study illuminated only collagen, there is little appreciation of the non-collagenous constituents of this region. However, the arrangement of the microstructure suggests a matrix for cellular and ground substance (that is, proteoglycans and hyaluronic acid) adhesion, conducive with minimally resistive biological surfaces. This is of importance clinically in maintaining the viability of the chondral surface. Deep to this, there is a loosely packed multidirectional fibrillar network. It could be hypothesized that this is able both to express fluid when loaded and to recover when unloaded in a viscoelastic manner. The labrum is also likely to be able to withstand excessive compression above a point at which fluid is expressed. In addition, this layer may tether the underlying structure together.

In contrast, the major component of the labrum is a core ring of densely packed circumferential tissue that might aid transfer of tensile forces resulting from both joint compression and translation of the humeral head, and therefore has an ability to decrease contact stress on the chondral surfaces by accommodating hoop stress.

Finally, the osseolabral transition zone incorporates a network of interdigitating anchoring fibres and Sharpey's fibres. The orientation and composition of these is seemingly random, particularly superiorly, suggesting that labral tethering is subjected to a number of multidirectional loads. Although this anchoring mechanism may not be significant in isolation, once the entire multidirectional network is recruited by load sharing through distribution of imposed stresses about the labral core hoop mechanism, the net effect may prevent translation. If this mechanism is flawed, or indeed the forces imposed exceed the limits of structural tolerance, the interface may fail. Whilst this commonly occurs clinically superiorly and anteriorly, manifest as a SLAP lesion or Bankart lesion, respectively, it is of importance to note that propagation of the latter of these lesions has been documented to occur on occasion through bone rather than the osseolabral interface, suggesting the tethering of the labrum is not mechanically insignificant (Burkhart & De Beer, 2000).

Specific to the labrum, Nishida et al. (1996) and Tamai et al. (1986) both hypothesized biomechanical properties

following their histological analysis of the labral collagen structure. The more recent study proposed that the mesh-like superficial layer absorbed compressive forces, whilst the stratified intermediate layer absorbed or dispersed different kinds of forces and the deepest layer acted as a main stabilizer (Nishida et al. 1996). The multidirectional fibres were thought to act as ties to resist circumferential splitting of the labrum by traction or compressive forces. Whilst plausible in the main, the superficial layer is unlikely to resist compression of the magnitude expected from the humeral head.

Tamai et al. (1986) proposed that the labrum is designed to withstand hoop tension due to the circumferential orientation of most of the fibres. They also considered that the radial fibres resisted forces acting to detach the labrum from the glenoid, and as such, the radial fibres are very sparse in contrast to the circumferential fibres, possibly making the labrum vulnerable to certain stresses (radial traction, compression, shear), whilst able to resist others (tensile; Tamai et al. 1986). Again, this is plausible. However, whilst composite mechanical properties resulting from collagenous orientations and conformations rely upon the integrity of the fundamental building blocks themselves, as isolated fibrillar properties contribute to an understanding of structural performance, the mechanical loading conditions are likely to require a complex synergy of responses to prevent failure. As such, the material composition of these structures is likely to be of importance.

Both circumferential and compressive collagenous elements demonstrated a significant amount of crimping, or kinking, on confocal microscopy, TEM and SEM. Simply, this may be due to the unloading of fibres under tension with a degree of elasticity. Equally, the crimp pattern seen may demonstrate compliance traits within the tissue (Parry & Craig, 1977); this mechanism has previously been observed in a number of connective tissues, such as tendons and ligaments (Butler et al. 1978).

Throughout the labrum, there are a number of collagen fibrils with differing cross-sectional diameters; indeed, there are some fibrils that have a different cross-sectional morphology. This may be suggestive of either different types of collagen present, or a function of maturity. Parry & Craig (1977) found a positive correlation between fibril size and the ultimate tensile stress of a tissue. In addition, Parry & Craig (1977) proposed that an increase in diameter of collagen fibrils leads to an increase in the potential density of intrafibrillar covalent crosslinks and therefore an increase in the tensile strength of the tissue. As such, the large number of wide fibrils in this study may indicate an ability of the labrum to accommodate significant loads. Furthermore, a decrease in fibril diameter leads to an increase in the density of interactions between collagen fibrils and the matrix, thus reducing the degree of non-recoverable creep, or viscoplastic deformation following mechanical loading of the tissue. Furthermore, different types of collagen have been proposed to possess different biomechanical properties (Kaltsas, 1983). Stellate and spiral fibrils have been detected in inherited connective tissue dysplasias such as Ehlers-Danlos syndrome (a disorder causing hyperextensibility and skin fragility; Ghadially, 1997), rheumatoid tissue (Neurath, 1993) and also in a previous study of shoulder and elbow capsules from normal subjects (Kaltsas et al. 1983), although no attempt to explain this finding was made. These abnormal morphologies are thought to arise as a result of a packing defect of the collagen filament in forming fibrils, or due to disaggregation of previously normal fibrils (Ghadially, 1997). Their presence in a disorder that results in hyperextensibility suggests that the labrum may have an elastic potential. However, the spiral and stellate fibrillar diameters in Ehlers-Danlos syndrome are unusually large (up to 500 nm; Vogel et al. 1979), whereas the fibrils in this study fall within the normal range of collagen fibrils. However, the disparity in results may be because this study measured minimum fibril diameters, whilst it is unclear what dimension was studied by Vogel et al. (1979). Both structural arrangements and material composition are useful tools in postulating physiological function and possible modes of failure. However, once failed, or indeed subject to altered mechanical demands, the structure must accommodate a remodelling mechanism to restore function.

The ability of the labrum to adapt through remodelling and repair itself once injured is imperative for the maintenance of stability. Cellular material, possibly fibroblastic, was noted throughout the tissue aligned along the length of fibres. It has previously been suggested that collagenous material remodels in response to changing mechanical environments and, as such, the presence of fibroblasts facilitates this process (Ohtani et al. 1988; Noorlander et al. 2002). The two cellular populations of the meniscus are fibrochondrocytes, able to synthesize a fibrocartilaginous matrix. The cellular material found in the glenoid is similar in morphology to that found in the deep meniscal tissue, tending to be round yet dendritic in appearance (McAlinden, 1998). As such, their biological role may be similar. Fibroblasts would not only facilitate remodelling, but also aid repair following a traumatic event. If the integrity of the labrum is disrupted, the distribution of loads would alter, and the tissue would remodel to incorporate this. This is of importance when planning surgery, as stability inferred through surgical repair of an unstable shoulder may later fail when the tissue has begun to reorganize to accommodate the imposed loading conditions more effectively.

Concluding remarks

The material properties of the glenoid labrum have been relatively unconsidered compared to the acetabular labrum and menisci of the knee. The results of this work and of some of the literature suggest that the glenoid

labrum is subjected to a number of mechanical environments. Possibly distinct regions of the labrum contribute to load sharing; a well vascularized hydrated compressive zone and a tensile component distributing circumferential hoop stress. Braiding and region interfaces suggest shear conditions.

Acknowledgements

We would like to acknowledge the technical expertise of Mr Stephen Rothery, Mr Ian Shore and Dr Robert Bielby in the preparation and imaging of the histological sections, and the kind support of Professor Nicholas Severs. Furthermore, we are grateful for the artistic support provided by Mr Juergen Hoerning. This work was supported by the Engineering and Physical Sciences Research Council and the Arthritis Research Campaign.

References

Bigliani LU, Pollock RG, McIlveen SJ, et al. (1995) Shift of the posteroinferior aspect of the capsule for recurrent posterior glenohumeral instability. *J Bone Joint Surg* **77-A**, 1011–1020.

Burkhart SS, De Beer JF (2000) Traumatic glenohumeral bone defects and their relationship to failure of arthroscopic Bankart repairs: significance of the inverted-pear glenoid and the humeral engaging Hill-Sachs lesion. *Arthroscopy* **16**, 677–694.

Butler DL, Groods ES, Noyes FR (1978) Biomechanics of ligaments and tendons. *Exerc Sport Sci Rev* **6**, 125.

Cooper DE, Arnoczky SP, O'Brien SJ, et al. (1992) Anatomy, histology, and vascularity of the glenoid labrum. An anatomical study. *J Bone Joint Surg* **74-A**, 46–52.

Fehringer EV, Schmidt GR, Boorman RS, Churchill RS, et al. (2003) The anteroinferior labrum helps center the humeral head on the glenoid. *J Shoulder Elbow Surg* **12**, 53–58.

Ferguson SJ, Bryant JT, Ito K (2001) The material properties of the bovine. acetabular labrum. *J Orthop Res* **19**, 887–896.

Ghadially FN (1997) *Ultrastructural Pathology of the Cell and Matrix*, 4th edn. Boston: Butterworth-Heinemann.

Gohlke F, Daum P, Bushe C (1994) [The stabilizing function of the glenohumeral joint capsule. Current aspects of the biomechanics of instability] *Z Orthop Ihre Grenzgeb* **132**, 112–119.

Habermeyer P, Schuller U, Wiedemann E (1992) The intra-articular pressure of the shoulder: an experimental study on the role of the glenoid labrum in stabilizing the joint. *Arthroscopy* **8**, 166–172.

Hertz H, Weinstabl R, Grundschober F, Orthner E (1986) Macroscopic and microscopic anatomy of the shoulder joint and the limbus glenoidalis. *Acta Anat* **125**, 96–100.

Hill AM, Jones IT, Hansen U, Suri A, et al. (2006) Treatment of ligament laxity by electrothermal shrinkage or surgical plication: a morphologic and mechanical comparison. *J Shoulder Elbow Surg* **16**, 95–100.

Huber WP, Putz RV (1997) Periarticular fiber system of the shoulder joint. *Arthroscopy* **13**, 680–691.

Kaltsas DS (1983) Comparative study of the properties of the shoulder joint capsule with those of other joint capsules. *Clin Orthop Relat Res* **173**, 20–26.

Levine WN, Flatow EL (2000) The pathophysiology of shoulder instability. *Am J Sports Med* **28**, 910–917.

Matsen F, Harryman D, Sidles J (1991) Mechanics of glenohumeral instability. *Clin Sports Med* **10**, 783–788.

McAlinden A (1998) The structure, biosynthesis and gene expression of extracellular matrix components in the human meniscus. PhD Thesis, Imperial College London.

Moseley HF, Övergaard B (1962) The anterior capsular mechanism in recurrent anterior dislocation of the shoulder. *J Bone Joint Surgery* **44-B**, 913–927.

Neurath MF (1993) Detection of Luse bodies, spiralled collagen, dysplastic collagen, and intracellular collagen in rheumatoid connective tissues: an electron microscopic study. *Ann Rheum Dis* **52**, 278–284.

Nishida K, Hashizume H, Toda K, et al. (1996) Histologic and scanning electron microscopic study of the glenoid labrum. *J Shoulder Elbow Surg* **5**, 132–138.

Noorlander ML, Melis P, Jonker A, Van Noorden CJ (2002) A quantitative method to determine the orientation of collagen fibers in the dermis. *J Histochem Cytochem* **50**, 1469–1474.

Ohtani O (1992) The maceration technique in scanning electron microscopy of collagen fiber frameworks: its application in the study of human livers. *Arch Histol Cytol* **55** (Suppl.), 225–232.

Ohtani O, Ushiki T, Taguchi T, Kikuta A (1988) Collagen fibrillar networks as skeletal frameworks: a demonstration by cell-maceration scanning electron microscope method. *Arch Histol Cytol* **51**, 249–261.

Owen GRh, Kääb M, Ito K (1999) Scanning electron microscopy examination of collagen network morphology at the cartilage, labrum, and bone interfaces in the acetabulum. *Scanning Microsc* **13**, 83–91.

Pagnani MJ, Warren RF (1994) Stabilizers of the glenohumeral joint. *J Shoulder Elbow Surg* **3**, 173–190.

Pagnani M, Deng X, Warren R, et al. (1995) Effect of lesions of the superior portion of the glenoid labrum on glenohumeral translation. *J Bone Joint Surg* **77-A**, 1003–1010.

Parry DA, Craig AS (1977) Quantitative electron microscope observations of the collagen fibrils in rat-tail tendon. *Biopolymers* **16**, 1015–1031.

Prodromos CC, Ferry JA, Schiller AL, Zarins B (1990) Histological studies of the glenoid labrum from fetal life to old age. *J Bone Joint Surg* **72-A**, 1344–1348.

Rao AG, Kim TK, Chronopoulos E, McFarland EG (2003) Anatomical variants in the anterosuperior aspect of the glenoid labrum: a statistical analysis of seventy-three cases. *J Bone Joint Surg* **85-A**, 653–659.

Tamai K, Okinaga S, Ohtsuka M, Inokuchi A (1986) Fibrous architecture of the glenoid labrum. In: *The Shoulder (Proc 3rd Int Conf Surg Shoulder)* (ed. Takagishi N), pp. 27–29. Fukuoka: Professional Postgraduate Services.

Vogel A, Holbrook KA, Steinmann B, et al. (1979) Abnormal collagen fibril structure in the gravis form (type I) of Ehlers-Danlos Syndrome. *Lab Invest* **40**, 201–205.

Wasserlauf BL, Matava MJ (2003) Advances in surgical management of superior labrum, anterior-to-posterior lesions. *Curr Opin Orthop* **14**, 262–268.

Williams PL, Bannister LH, Berry MM, et al. (1995) *Gray's Anatomy*, 38th edn, New York: Churchill Livingstone.